19

Kikuchi Diffraction

CHAPTER PREVIEW

In this chapter and the following two, we will discuss two special cases of electron diffraction. We'll see that incoherently scattered, divergent beams of electrons give rise to paired arrays of lines in SADPs, known as Kikuchi patterns. In the next two chapters, we will form DPs with a convergent rather than a divergent (or, as in the previous chapter, parallel) beam. These two techniques have a lot in common. In the first, the electrons are initially being scattered by the atoms in the crystal so that they 'lose all memory of direction' and may also lose energy. We can then think of these electrons as traveling in diverging 'incident' directions into the specimen. When the direction is appropriate, these electrons can be scattered again, this time by Bragg diffraction. In the second technique, we intentionally form a convergent beam in the illumination system to make the electrons incident on the crystal over a range of different angles and create convergent-beam electron diffraction (CBED) patterns. In this case, we have another advantage in that we can focus the beam on a much smaller area of the specimen than in SAD. In both cases the information gained is enhanced if the specimen is thicker; in the case of Kikuchi patterns it has to be thick enough for inelastic scattering to occur and in CBED it has to be thick enough for dynamical scattering. So these next three chapters are particularly useful if you can't make your specimen thin enough for almost all other TEM techniques, which generally produce better quality information if the specimen is thinner.

In this chapter, we will show that these Kikuchi patterns can be used to give us much more accurate information on the beam direction than SADPs and can also give a direct link in reciprocal space to the stereographic projection. The topics we'll cover are basically experimental (although the phenomenon is well understood theoretically) and software for computer simulation of Kikuchi patterns is readily available and very useful. The ideas we develop in this chapter will carry over to the next two chapters when we discuss higher-order Laue-zone (HOLZ) lines in CBED patterns (where Kikuchi lines can also appear).

19.1 THE ORIGIN OF KIKUCHI LINES

The reason Kikuchi patterns form is that, if the specimen is thick enough, it will generate a large number of scattered electrons which travel in all (but mainly forward) directions; i.e., they have been *incoherently* scattered but not necessarily *inelastically* scattered (although obviously some of them will have lost energy). They are sometimes referred to as diffusely scattered electrons. These electrons can then be Bragg diffracted by the crystal planes. The rest of the story is merely geometry.

We'll discuss a little of the theory in Section 19.5, but for now we'll note the following experimental facts

- Since typical energy losses are small (15–25 eV) compared to E_0 (100–400 keV) the diffusely scattered electrons can be assumed to have the same λ as the incident electrons. This assumption holds as long as the specimen is not too thick.
- When first formed, most of the diffusely scattered electrons travel close to the direction of the incident beam. You learned back in Chapter 3 that inelastic scattering is 'peaked in the forward direction.'

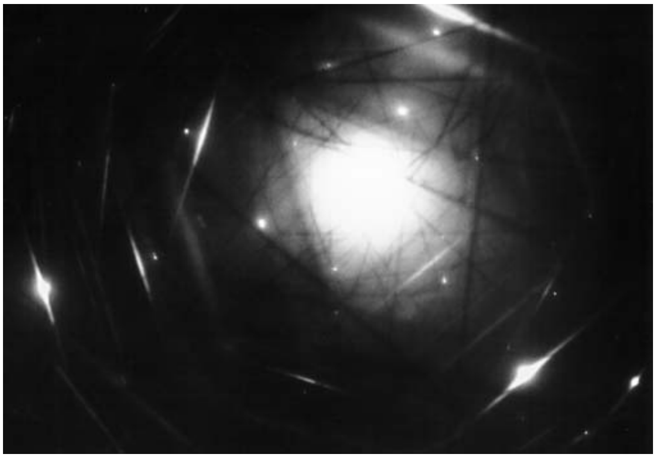

FIGURE 19.1. An ideal DP containing both well-defined spots and clearly visible pairs of bright (excess) and dark (deficient) Kikuchi lines.

- The ideal specimen thickness will be such that we can see both the spot pattern and the Kikuchi lines as illustrated in Figure 19.1. As noted, this is one of the few situations when thinner is not necessarily better.
- Although this phenomenon is related exclusively to electron scattering, Kikuchi described it in 1928, *before* the development of the TEM; it can occur in any crystalline specimen.

Diffuse scattering will again be important when we discuss forming images from these electrons in Section 31.5. We can select a region of reciprocal space containing diffusely scattered electrons to form the image and these electrons can be separated from the inelastically scattered electrons with an energy filter (see Sections 38.2 and 40.5). Your specimen needs to be thick enough but, if it is too thick, then there will be no Kikuchi lines because inelastic scattering then dominates and there is no detectable Bragg diffraction of these electrons. There will also be no Bragg spots and no useful DP!

19.2 KIKUCHI LINES AND BRAGG SCATTERING

The geometry of Kikuchi patterns can be understood from Figure 19.2 which relates what happens in the specimen to what we see in the DP. Let's imagine (Figure 19.2A) that electrons have been generated at the point shown and are scattered in all directions (but

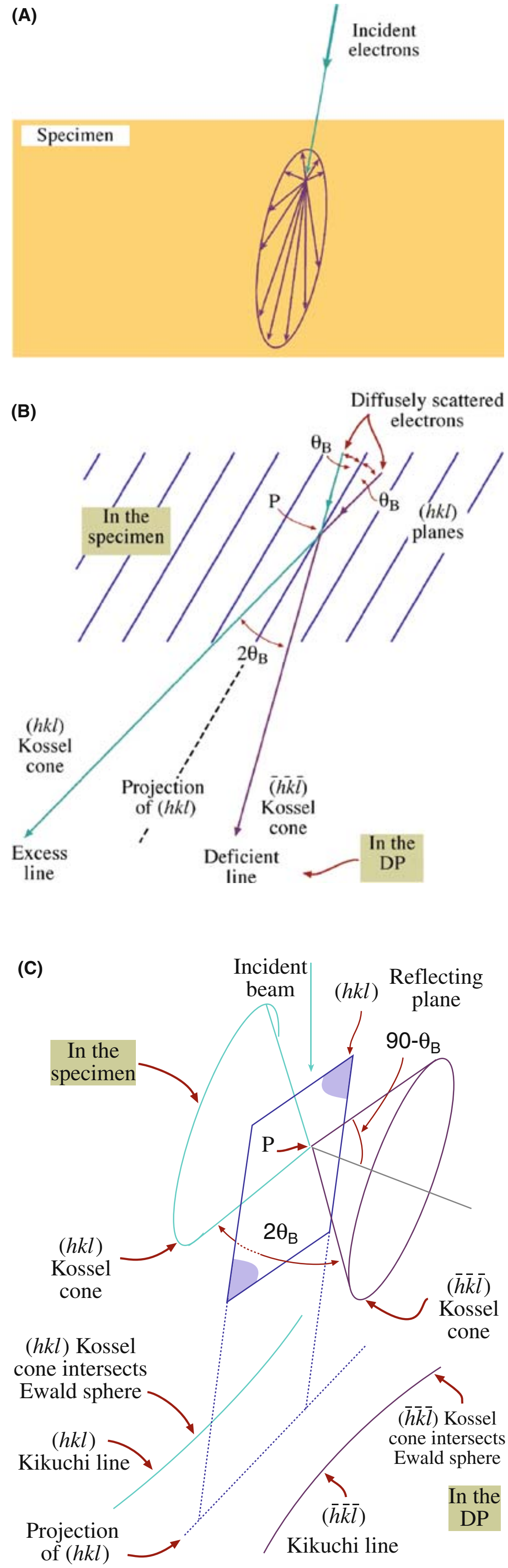

FIGURE 19.2. (A) Schematic representation of all electron scattering localized at a single point in the specimen. In (B) some of the scattered electrons are diffracted because they travel at the Bragg angle θ_B to certain *hkl* planes. The diffracted electrons form Kossel cones centered at P on the diffracting planes. The lines closest to the incident beam direction are dark (deficient) and the lines farthest away are bright (excess). In (C) the cones intercept the Ewald sphere, creating parabolas which approximate to straight lines in the DPs because θ_B is small.

mainly forward). So we draw them as diverging from a point even though, in fact, they'll be scattered at different points throughout the specimen thickness. Some of these electrons will travel at an angle θ_B to the *hkl* planes as shown in Figure 19.2B and then be Bragg diffracted by these specific planes. Since the scattered electrons are traveling in all directions, the diffracted beam will lie on one of two cones (Figure 19.2C). In other words, we see cones of diffracted electrons rather than well-defined beams because there is a *range* of incident **k**-vectors rather than a single **k**-vector. We construct the cones by considering all the vectors oriented at angle θ_B to the *hkl* plane; these are called Kossel cones and the cone angle (90–θ_B) is very small (remember, angle really means semi-angle). There is a pair of Kossel cones for $\pm\mathbf{g}$, another pair for $\pm 2\mathbf{g}$ and so on.

SEEING KOSSEL CONES

What we see in the DP is the intersection of these two cones with the screen or detector.

Since the screen/detector is flat and nearly normal to the incident beam, the Kossel cones appear as parabolas. If we consider regions close to the optic axis, these parabolas appear as two parallel lines. (Remember how close to 90° the cone angle is.) We'll sometimes refer to this pair of Kikuchi lines as a 'Kikuchi band' to include the lines and the region between them; the contrast associated with the region between the lines is actually quite complex (Section 19.6).

FOR ANY PAIR OF KIKUCHI LINES

One line corresponds to θ_B and the other to $-\theta_B$; one is the **g** Kikuchi line and the other the $\bar{\mathbf{g}}$ Kikuchi line. *Neither* of them is the **0** Kikuchi line.

We can make another important observation on the intensity of these lines by considering Figure 19.2 again. In Figure 19.2B you can see that the scattered beam which was initially closest to the optic axis, and therefore the more intense, is farther away from the axis after being Bragg diffracted. This beam then gives the excess (bright) line and the other the deficient (dark) line. You can see that this simple idea really does work in Figure 19.1.

The value of this result comes when we want to index a pair of Kikuchi lines: if you find a bright line, its partner must not only be parallel to it but must also be closer to O, and dark. The pair is separated by $2\theta_B$.

The cones shown in Figure 19.2C act as if they are rigidly fixed to the plane *hkl*; they are thus 'fixed' to the crystal. We can draw a line half way between the two Kikuchi lines to represent the trace of the plane (*hkl*). Remember our angles are all small. This simple observation explains why we have a whole chapter on Kikuchi lines.

TILTING AND KIKUCHI LINES

If we tilt the crystal through a very small angle, the Kikuchi lines will move but the intensities of the diffraction spots will hardly change and the positions of the spots will not change. So Kikuchi lines are much more sensitive to beam/specimen tilts than spots in SADPs.

The location of the Kikuchi line will also tell us whether **s** is positive or negative. We can't usually deduce that from the spot pattern.

The distance in reciprocal space between the $\bar{\mathbf{g}}$ and **g** Kikuchi lines is **g** (not 2**g**) because the angle between the two Kossel cones is $2\theta_B$. This relationship is very valuable for the following reasons

- When the **g** Kikuchi line passes through the reflection G, $\mathbf{s_g} = 0$ (i.e., the Bragg condition is exactly satisfied) and the $\bar{\mathbf{g}}$ Kikuchi line passes through O. So we can use the Kikuchi lines to set up specific diffraction conditions exciting specific reflections as we tilt the specimen (see Figure 19.3). We'll see later that we can also use Kikuchi lines to determine the exact value of $\mathbf{s_g}$ when we are close to, but not exactly at, an exact Bragg condition.
- A corollary: if the direct beam is exactly parallel to the plane *hkl*, the **g** and $\bar{\mathbf{g}}$ Kikuchi lines are symmetrically displaced about O with the **g** Kikuchi line 'passing through' **g**/2 and the $\bar{\mathbf{g}}$ line 'passing through' $\bar{\mathbf{g}}$/2.

In this latter case, our simple explanation of Kikuchi-line formation breaks down, because Figure 19.2 predicts equal intensity in both excess and deficient Kikuchi lines and they would both, therefore, be indistinguishable from the diffuse-scattered background. So no Kikuchi lines should be visible if the beam is exactly down a zone axis, and this is patently not true. So the full Kikuchi-line explanation is more complex and (unfortunately) requires Bloch-wave theory. But we do understand the process in great detail.

19.3 CONSTRUCTING KIKUCHI MAPS

If instead of just taking pictures of Kikuchi-line pairs, we assemble a montage of all Kikuchi lines and spot patterns

KIKUCHI MAP

Making a Kikuchi map is a highly recommended exercise if you are going to be doing detailed diffraction-contrast images/SAD experiments because familiarity with the Kikuchi map will help you to immediately identify the orientation of your specimen on your TEM screen.

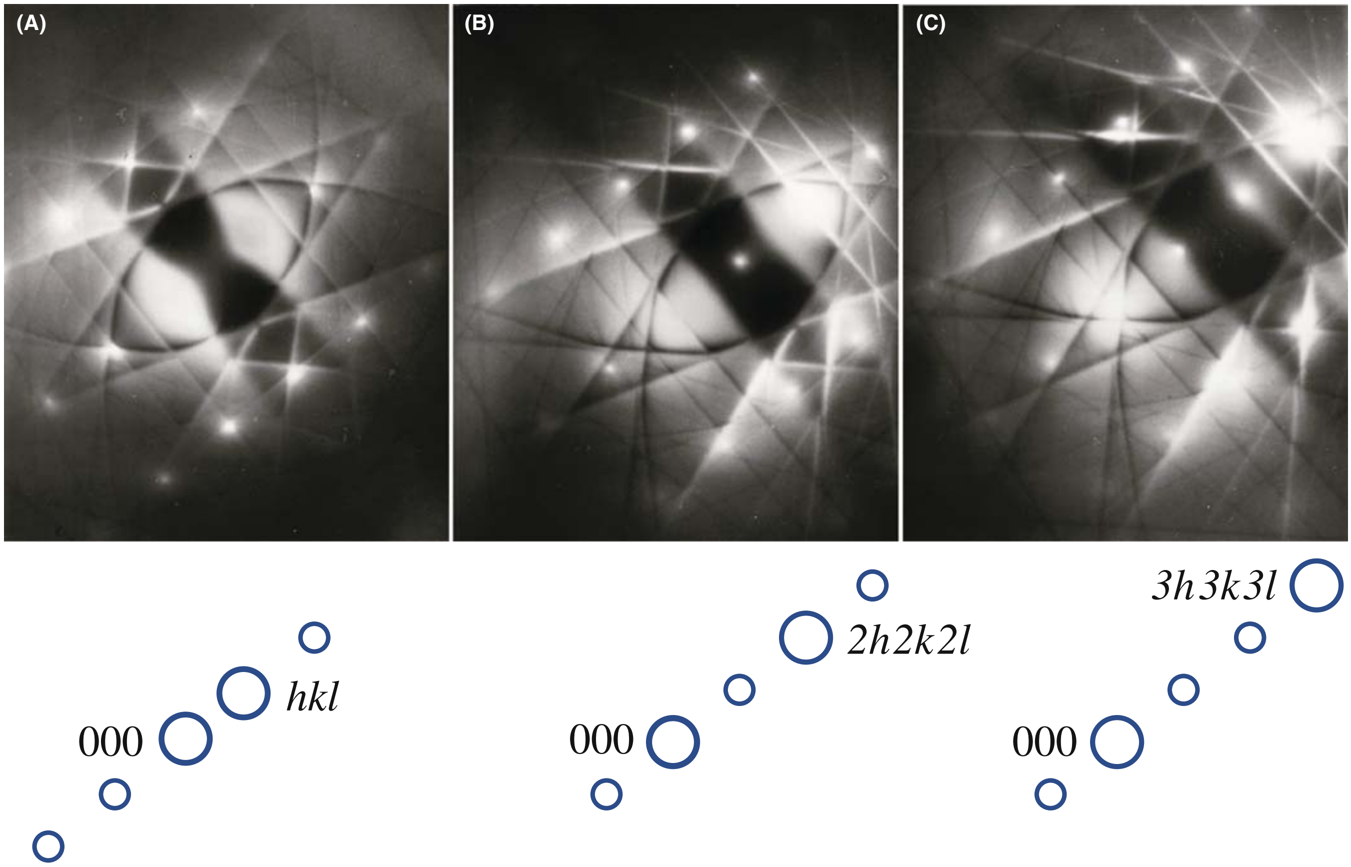

FIGURE 19.3. Three two-beam DPs from pure Al, obtained under different tilting conditions. As shown schematically below each figure, in (A) the *hkl* spot is at the exact Bragg condition (the excess Kikuchi line goes through *hkl*). In (B) the *2h2k2l* and in (C) the *3h3k3l* spots, respectively, are strongly excited. Note that although we refer to these as 'two-beam' DPs, many other diffraction spots are visible.

over a wide array of reciprocal space, then we create a Kikuchi map.

The method for constructing Kikuchi maps is illustrated in Figure 19.4A. First, we draw the lines for the case where the [001] pole is exactly on the optic axis. The lines are then the perpendicular bisectors of every **g**-vector you can find in the ZOLZ. The distance between each pair of lines is then automatically |**g**|. We can then give each line a unique label **g**.

Next, we can construct the map for the [101] pole. We start as shown in Figure 19.4B, keeping the common 020 **g**-vector pointing in the same direction. So, the 020 and $0\bar{2}0$ Kikuchi lines are common to the two patterns. Although the angle between the [001] and [101] poles is 45°, we draw the 020 lines as parallel and straight because we are always looking at a small segment of the Kikuchi pattern. Notice that we can define all the distances in terms of their equivalent angles, as in any DP.

Now we add the [112] pattern. This pattern shares the $2\bar{2}0$ and $\bar{2}20$ reflections with the [001] pole and shares the $\bar{1}\bar{1}1$ and $11\bar{1}$ reflections with the [101] pole. The corresponding pairs of Kikuchi lines will then also be common, so we produce the triangle shown in Figure 19.5A. We can add other poles and pairs of Kikuchi lines as shown in Figure 19.5B to get the full pattern.

A Kikuchi map for an fcc material is illustrated in Figure 19.6. The maps are available in the literature for fcc, bcc, diamond cubic and some hcp materials. Such maps are mainly from Thomas and co-workers (Levine et al. 1966, Okamoto et al. 1967, Johari and Thomas 1969), who developed the technique. Edington (1976) presents several Kikuchi maps in the appendices. Maps can also be downloaded from the Web using EMS (URL #1).

You can appreciate the value of Kikuchi maps in noncubic materials from the map shown in Figure 19.7. The map has been drawn for Ag_2Al, which has the same c/a ratio as Ti. The Kikuchi bands are labeled (remember that they correspond to planes). The zone axes are also labeled: they correspond to directions. Thinking back to our brief discussion of Frank's paper on four-index notation in Chapter 16, you should see an obvious application here.

- For cubic materials you need only the [001], [101], [111] triangle shown in Figure 19.5B.
- For hcp materials, the angles will generally depend on the c/a ratio of your material and you'll need a larger area of the map.

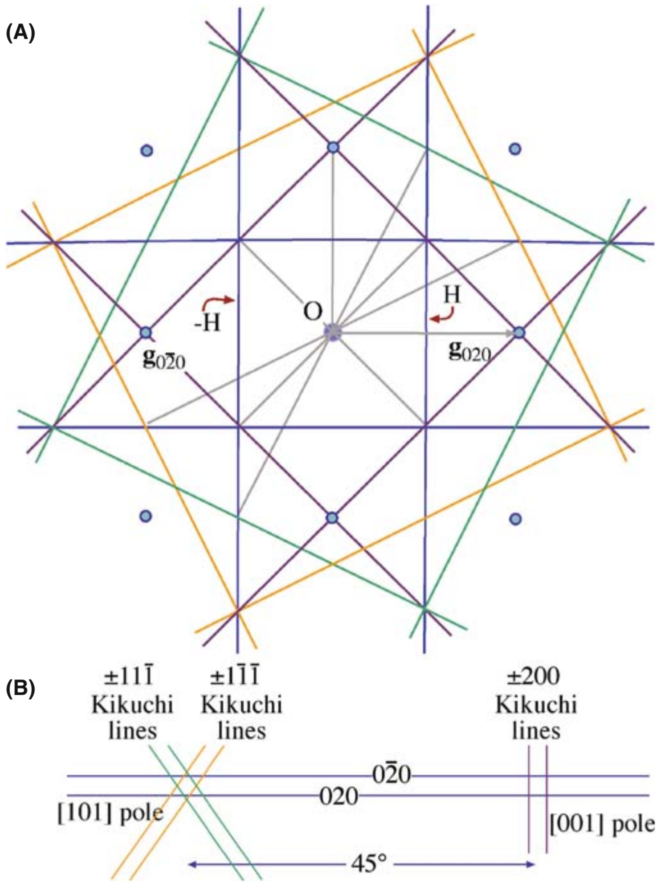

FIGURE 19.4. (A) To construct a Kikuchi pattern, draw pairs of lines each bisecting the ±**g**-vectors. For example, when the [001] fcc pole is on axis, the vector $\mathbf{g}_{020}$ is bisected by the vertical line at H (020); the other Kikuchi line in the pair is at −H (020). All other Kikuchi-line pairs can be constructed for any **g**-vector. (B) From one Kikuchi pattern we can extend the lines to create a second pattern. For example, knowing the [001] pattern we can construct the [101] pattern since a pair of lines is common to both. So we draw the 0$\bar{2}$0 and 020 lines from the [001] pole 45° to the [101] pole.

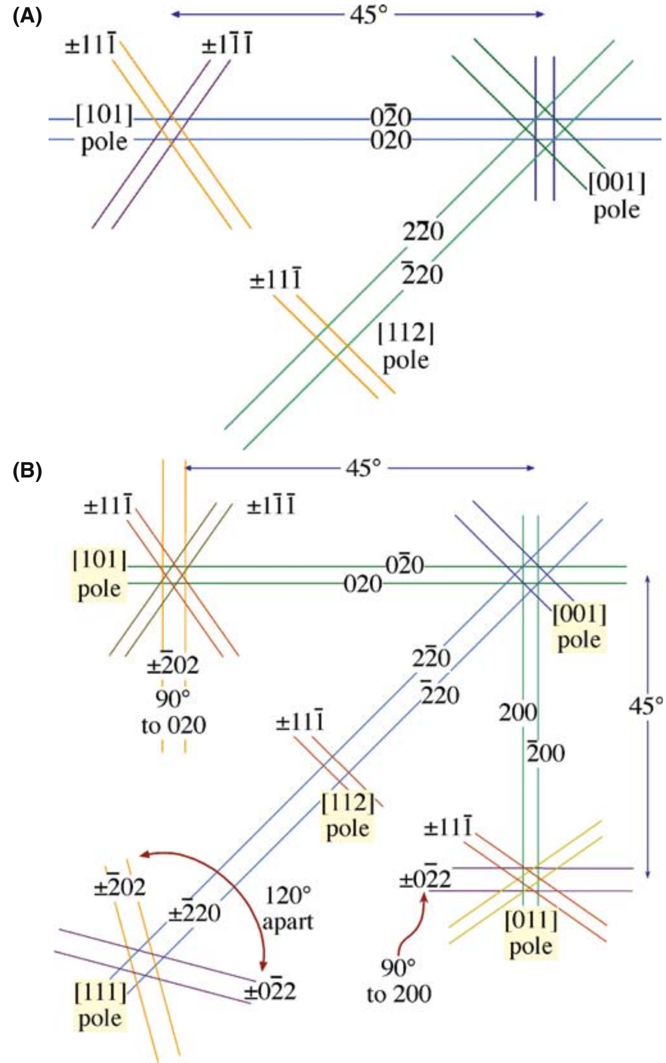

FIGURE 19.5. (A) Construction of the [112] pattern from the [001] and [101] patterns by extending the Kikuchi lines common to each pair of patterns. The [111] pair is common to the [001] and [112] patterns and the $\bar{2}$20 pair is common to [001] and [112] patterns. (B) Other poles can be added such as [011] and [111]. Note that the Kikuchi-line pairs are not straight lines connecting poles. They are curved because over large angles their parabolic shape is evident. Nevertheless we draw them as straight lines where possible.

- For most non-cubic materials and particularly if you are working with monoclinic or triclinic crystals, it's not practical to construct the complete map experimentally. It's probably easier to become a metallurgist!

We can use the following procedure to generate a valuable experimental aid for any material.

- Construct segments of the map to scale as we've illustrated in Figure 19.5B. You can use one of the software packages to help you in this task. Make two copies of each map.
- While you're at the TEM, record the Kikuchi pattern for several special low-index poles along with the spot pattern.
- Index the DPs consistently.
- Print both DPs for each zone axis at the scale you used in your line drawing of the Kikuchi map.
- Now add the experimental patterns to the line diagrams and you have two very useful experimental aids. An illustration is given in Figure 19.8.

When discussing Kikuchi maps, we like to use the road-map analogy. (Repeatedly!) What we just recommended is that you record the maps of the towns with pictures so that you'll recognize them. When you're on the highway traveling from town to town, you don't much care what the road looks like although you do want to know how far you've traveled and how much farther you have to go.

By now you will appreciate even more the value of the stereographic projection we introduced in Chapter 18.

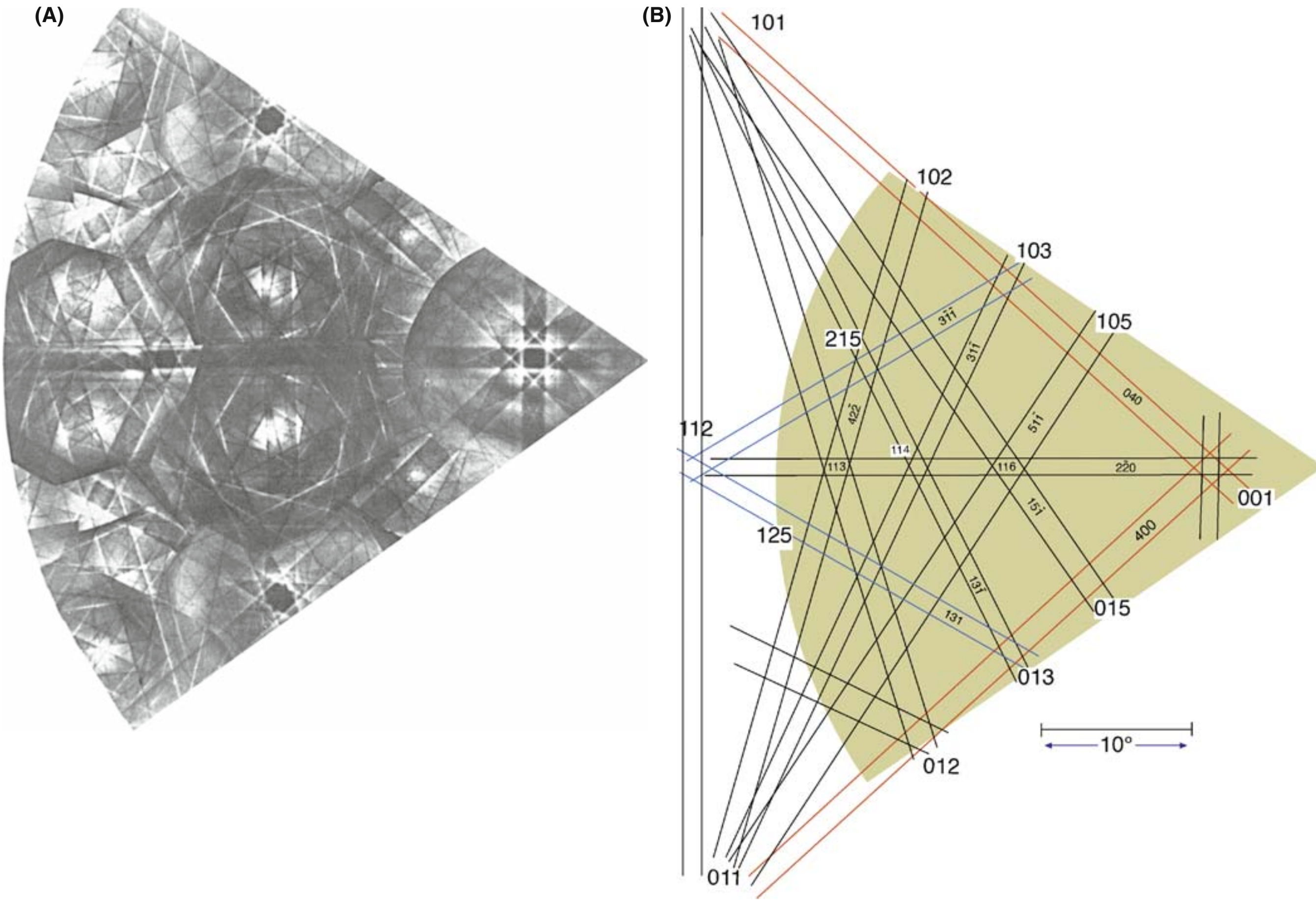

FIGURE 19.6. (A) Experimental Kikuchi map for fcc crystals and (B) indexed Kikuchi lines in the schematic map.

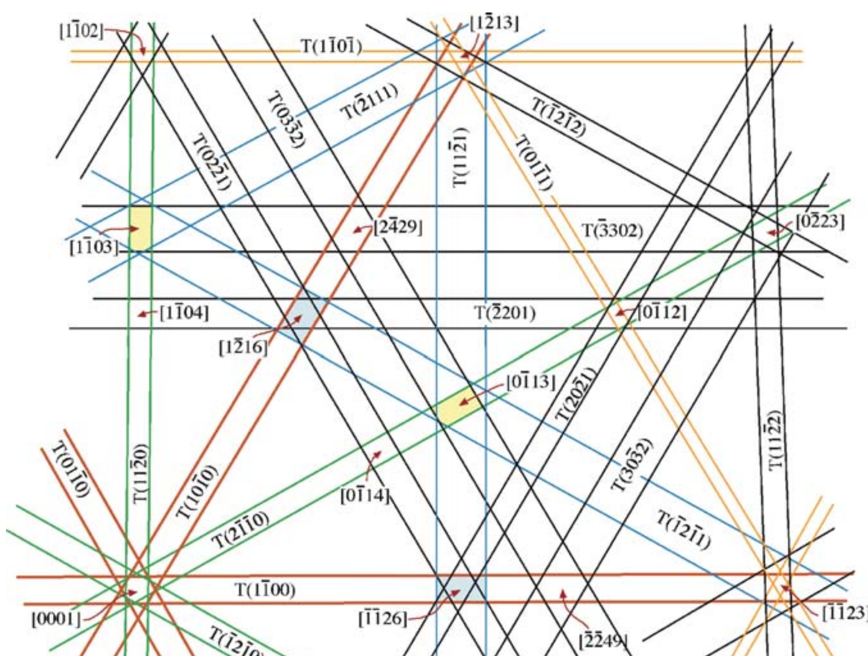

FIGURE 19.7 Part of the Kikuchi map for hexagonal Ag_2Al with the principal poles and pairs of lines indexed.

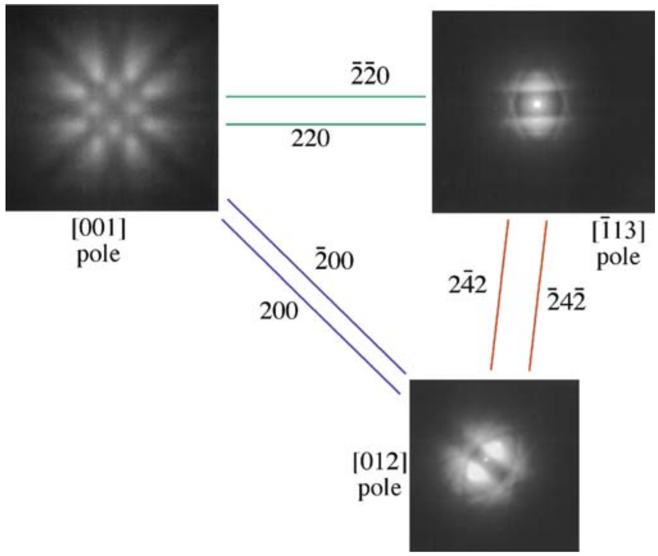

FIGURE 19.8. Experimental Kikuchi patterns around three principal poles in MgO with the common Kikuchi lines between each pole drawn in. You should compare this figure with the DPs in Figure 18.7.

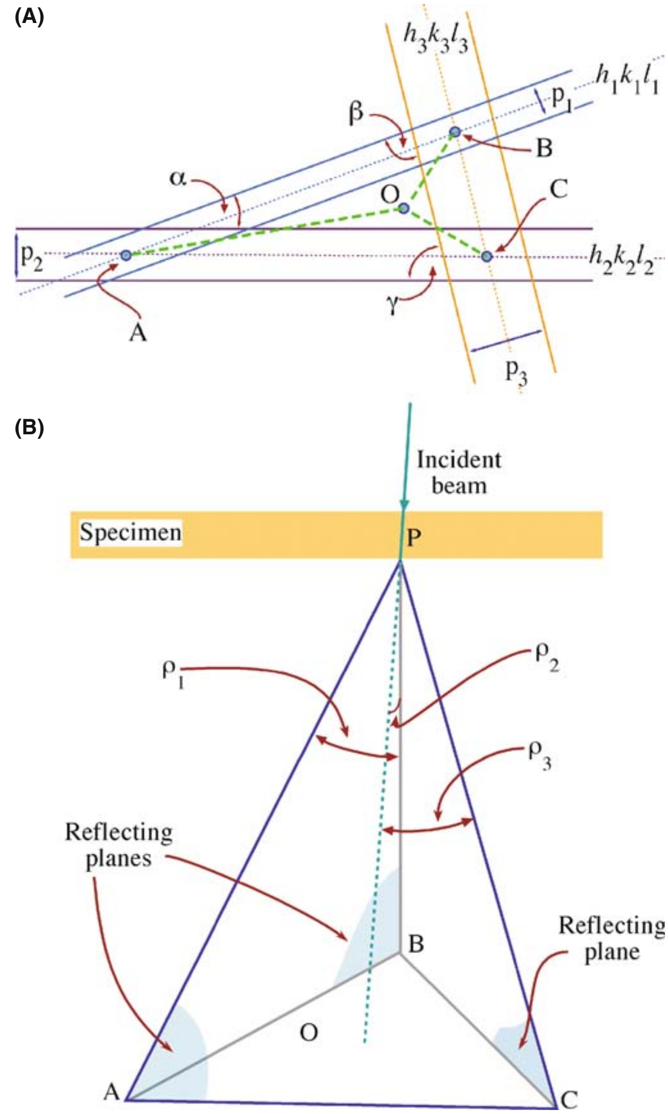

FIGURE 19.9. In (A) pairs of Kikuchi lines from the reflecting planes also intercept at points A, B, C. The distances from O to the points A, B, C correspond to the angles between the beam direction and the three zone axes while the angles α, β, γ correspond to the angles between pairs of plane normals. The angle α is between the ($h_1k_1l_1$) and ($h_2k_2l_2$) plane normals, etc. (B) Three reflecting planes in the specimen with traces AB ($h_1k_1l_1$), AC ($h_2k_2l_2$) and BC ($h_3k_3l_3$), around the direct beam, O; the traces of pairs of planes intercept at A (AB, AC), B (AB, BC) and C (AC, BC).

Use the stereographic projection and the Kikuchi map together. The stereographic projection concisely summarizes all the relative locations of all the plane normals and the zone axes. Use the stereographic projection to relate Storrs and Huntsville, but use the Kikuchi map to locate the Benton Museum of Art and the Von Braun Center.

19.4 CRYSTAL ORIENTATION AND KIKUCHI MAPS

In the previous chapter we showed how you could use SADPs to estimate the orientation of the beam relative to the crystal with an accuracy of ±3°. Using Kikuchi patterns you can increase this accuracy to ±1°.

A routine method for orientation determination was developed by Thomas and co-workers (e.g., Okamoto et al.); they pioneered the use of Kikuchi maps in TEM analysis. The beam direction [*UVW*] lies along the optic axis O in Figure 19.9. A, B and C are major poles (i.e., zone axes) which we can determine by observation and measurement. Let the indices of A = [p_1 q_1 r_1], B = [p_2 q_2 r_2] and C = [p_3 q_3 r_3]. Having indexed these poles, we can check our result by measuring the angles α, β and γ between the traces of the planes in Figure 19.9A (which equals the angle, ϕ, between the plane normals in all systems); we must calculate each angle using equation 18.3 if the specimen is cubic.

SPECIMEN ALIGNMENT
Kikuchi lines transform SADPs from an approximate to a very precise alignment technique.

If we measure the distances OA, OB and OC in Figure 19.9A, we can convert them into angles ρ_1, ρ_2 and ρ_3 (which are defined in Figure 19.9B) by using our calibrated camera length. If [*UVW*] is the direction of the beam, then we can use the same vector-dot-product approach (equation 18.4 for the cubic case) to give equations for ρ_1, ρ_2 and ρ_3. Notice we are distinguishing between ρ and ϕ (see Section 18.4). The angles α, β and γ in Figure 19.9A are slightly distorted values of (90 – ϕ).

We can solve these three equations for the three unknowns *U*, *V* and *W* and hence we have **B**. Finally, you should always check the sign of **B**, as we described in Section 18.10.

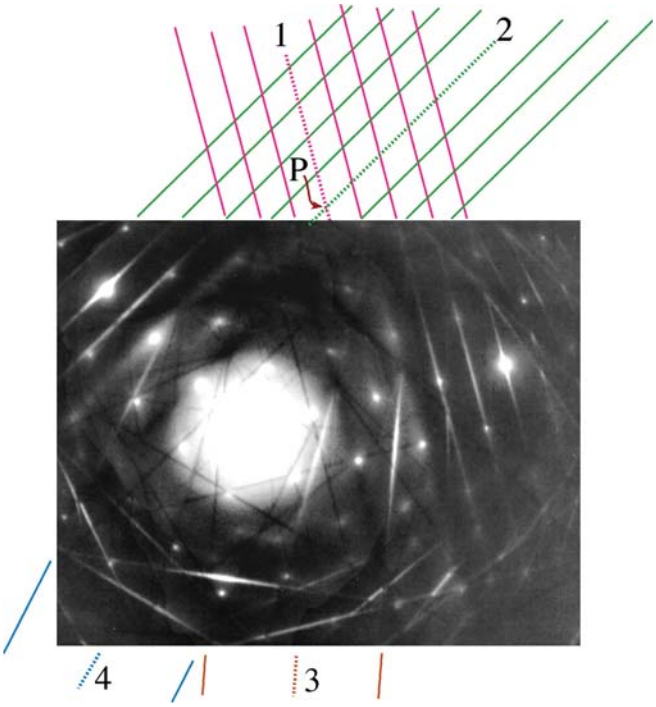

FIGURE 19.10. To index a DP well away from a low-index zone axis, extend the Kikuchi lines. The dark lines 1–4 represent the traces of the diffracting planes which intercept at a pole (P). For Kikuchi lines 1 and 2, the higher-order extensions are also drawn. From the *d*-spacings, index the Kikuchi-line pairs. The angles between the beam direction and the poles, P, can then be measured directly.

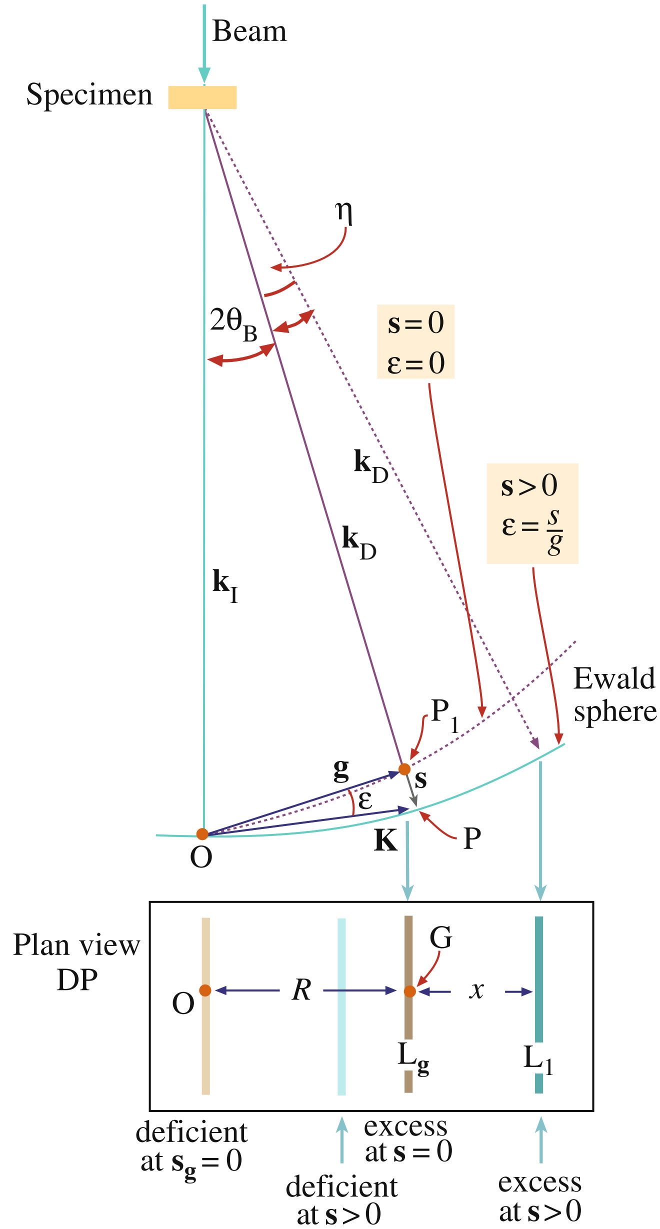

FIGURE 19.11. The distance between the diffraction spot and its Kikuchi line gives a direct measure of **s**. The angle ε is s/g and is zero at the exact Bragg condition. In the box: measure *x*, the spacing between O and the deficient line (or G and the excess line) to determine **s**.

It is possible that the DP you have to work with is not obviously near a zone axis. All is not lost if you can just find pairs of Kikuchi lines as shown in Figure 19.10. If you see an excess line you will find the deficient line quite easily, closer to 000. Now trace these lines in both directions and you have found the poles. Use your knowledge of the *d*-spacings to index the pairs of Kikuchi lines. Remember that the zone axis lies parallel to each plane so it's defined by where the two plane traces meet. Now, if you can index three poles, you can obtain **B** as in Figure 19.9.

DO REAL-TIME CRYSTALLOGRAPHY

Normally, while you are at the TEM, tilt along the different Kikuchi bands until you find the appropriate poles to ease your task later.

19.5 SETTING THE VALUE OF S_g

Since the Kikuchi lines are 'rigidly attached' to the crystal, they give us a very accurate measure of the excitation error $\mathbf{s_g}$. The diffraction geometry is shown in Figure 19.11 following Okamoto et al. When $\mathbf{s_g}$ is negative, the **g** Kikuchi line is on the same side of **g** as O; when $\mathbf{s_g}$ is positive, the line lies on the opposite side of **g**. If you look at Figure 19.10 you'll see that the bright diffraction spot at the top LH corner of the DP is under $\mathbf{s_g}$ positive conditions (excess Kikuchi line outside the spot), the bright spot at the middle/upper RH side is under $\mathbf{s_g}$ zero conditions (the excess Kikuchi line through the spot) and the bright spot toward the bottom of the DP is under $\mathbf{s_g}$ negative conditions (the excess Kikuchi line inside the spot).

For high-energy electrons, and knowing the camera length *L*, we can write an expression for the angle η in Figure 19.11

$$\eta = \frac{x}{L} = \frac{x\lambda}{Rd} \tag{19.1}$$

where d is $|\mathbf{g}|^{-1}$. The distances x and R are measured on the photographic negative.

The angle ε is given by

$$\varepsilon = \frac{s}{g} \tag{19.2}$$

Now we can set $\varepsilon = \eta$ to give

$$s = \varepsilon g = \frac{x}{L} g = \frac{x}{Ld} \tag{19.3}$$

Again, with our small-angle approximation, the distance between the excess and deficient Kikuchi lines, R (the distance g measured on the DP), is equivalent to $2\theta_B L$. So, using Bragg's law, we have

$$\frac{R}{L} = 2\theta_B = \frac{\lambda}{d} \tag{19.4}$$

Hence the expression for s is

$$s = \frac{x}{Ld} = \frac{x}{d} \cdot \frac{\lambda}{Rd} \tag{19.5}$$

$$s = \frac{x}{R} \frac{\lambda}{d^2} = \frac{x}{R} \lambda g^2 \tag{19.6}$$

We'll reconsider this equation when we discuss weak-beam microscopy in Chapter 27.

Ryder and Pitsch have given a method for determining **B** using the approach we described in Section 19.4 with the accuracy given by equation 19.6. Their expression for **B** is

$$\mathbf{B} = \alpha_1 |\mathbf{g}_1|^2 (\mathbf{g}_2 \times \mathbf{g}_3) + \alpha_2 |\mathbf{g}_2|^2 (\mathbf{g}_3 \times \mathbf{g}_1) + \alpha_3 |\mathbf{g}_3|^2 (\mathbf{g}_1 \times \mathbf{g}_2) \tag{19.7}$$

where α_i is given by

$$\alpha_i = \frac{R_i + 2x_i}{R_i} \tag{19.8}$$

where R and x are defined in Figure 19.11.

19.6 INTENSITIES

We'll conclude with a few remarks for further thought

- Tan et al. have shown experimentally that the distance between a pair of Kikuchi lines may change at larger specimen thicknesses due to dynamical scattering.
- Kikuchi lines can also be produced by the backscattered electrons. In the SEM these patterns are termed electron-backscatter DPs (sometimes EBSPs) and the technique as EBSD. They were regarded as a curiosity until it was shown (see Dingley's paper) that you can map out the texture of polycrystalline materials using these patterns, without thinning the sample. Not much happened for a decade or more until new detection systems, using CCD cameras and fast computer algorithms led to the development of orientation imaging microscopy (OIM) (see Dingley's review). As we saw in Section 18.13, similar techniques are available for automatic indexing of TEM DPs and Kikuchi maps. They aren't as automated, nor can they index as many patterns as EBSD software because there are usually far fewer thin grains in our specimens than crystals in an SEM specimen. But TEM can, in principle, give the interface plane much more accurately, so the two techniques will become more complementary with time.
- In the next chapter, we'll discuss HOLZ lines; HOLZ lines are very closely related to Kikuchi lines but are a little more complicated, since the Bragg planes are always inclined to the direct beam.
- In Chapter 24, we'll discuss ZAPs, or zone-axis patterns, in *images*; these ZAPs are, in many respects, the real-space version of Kikuchi lines. However, you'll see that their physical origin is *completely different*; the most important features of ZAPs are *not* associated with incoherent, inelastic or diffuse scattering.
- Bloch waves with vector $\mathbf{k}^1$, for example, are more strongly scattered than those corresponding to branch 2 of the dispersion surface. Therefore, we can expect anomalous absorption (see Chapter 24) to influence the intensity of Kikuchi patterns. Such effects do in fact lead to excess and deficient Kikuchi bands. Since we haven't yet found any use for the information in these bands we'll leave them as an exercise for further reading!
- We mentioned earlier that the contrast between the Kikuchi lines, i.e., the Kikuchi band, is complex. The contrast is strongly influenced by anomalous absorption of the Bloch waves which are formed by coherent scattering of the incoherently scattered electron, so all is clear.
- There are strong similarities between the Kikuchi process and the operation of a monochromator in optics: both select and diffract a particular wavelength or frequency.
- You can appreciate that the scattering is quite complex by considering what happens when the diffracting plane is exactly parallel to the incident beam: as we've mentioned, the two Kikuchi lines will both be visible although you might have guessed otherwise.

Back in Chapter 6 we noted that electron ray paths rotate through the objective-lens field, but in all our discussion on diffraction (including Kikuchi lines and the CBED patterns in the next two chapters) we draw all the electron paths as straight lines, ignoring any rotation. However, particularly in a modern condenser-objective lens TEM, the lens field is relatively strong and can introduce a significant rotation into the off-axis incident and diffracted electrons (we described c/o lenses and their effects on ray paths back in various sections of Chapter 9). An interesting consequence of this effect is that Kikuchi lines in modern TEMs may be less sharp than in older TEMs, unless you illuminate only a very small area of the specimen. If you're intrigued by this problem then you must read "Skew thoughts on parallelism" by Christenson and Eades.

CHAPTER SUMMARY

Pairs of Kikuchi lines define the road and, taken together, the roads make up a map of reciprocal space. However, the key is different from real-space road maps because in our Kikuchi maps, narrow roads are the most important! What is the relevance of the roadside curbs? Well, they define the roads and tell us when we are standing on them, but we are not too interested in their detailed appearance. You should by now be under the (correct) impression that we view Kikuchi lines and maps as an invaluable tool for the microscopist. The key points are

- The Kikuchi lines arise from Bragg diffraction of divergent, incoherent electrons scattered within the specimen.
- The Kikuchi lines consist of an excess (bright) line and a deficient (dark) line. In the DP, the excess line is farther from the direct beam than the deficient line.
- The Kikuchi lines are effectively fixed *to the crystal* so we can use them to determine orientations accurately.
- The trace of the diffracting planes is midway between the excess and deficient lines.
- We can use the Kikuchi lines to set up specific (e.g., two-beam) diffracting conditions which are central to diffraction-contrast imaging.
- We can control and determine the value of $\mathbf{s_g}$ by measuring the separation between the **g** Kikuchi line and the G reflection (the separation is 0 when $\mathbf{s_g} = 0$). The precise value of $\mathbf{s_g}$ is also very important in controlling diffraction contrast.

Kikuchi lines and maps are two of the most important aids you have when orienting (or determining the orientation of) crystalline specimens. Knowing the orientation of your specimen is essential for any form of quantitative TEM, whether you're analyzing dislocation Burgers vectors by diffraction contrast, imaging grain boundaries with lattice resolution or measuring chemistry variations by EELS or XEDS. Kikuchi maps are especially useful when combined with the map of zones and poles (directions and plane normals) on the stereographic projection. Use a computer to check or to assist you in constructing such a map for your material but if you're doing any serious crystallography, never leave home or sit at your TEM without a map to guide you.

IN GENERAL

Edington, JW (1976) *Practical Electron Microscopy in Materials Science*, Van Nostrand-Reinhold New York. Part 2 of the book is still an excellent source of guidance if you are doing hands-on DP acquisition and analysis and the Appendix has great Kikuchi maps.

Schwartz, AJ, Kumar, M and Adams, BL (Eds.) (2000) *Electron Backscatter Diffraction in Materials Science*, Springer NY. Kikuchi patterns in the SEM: an insight into what could really be done in terms of orientation determination in TEM, if we put our minds to it.

Thomas, G (1978) in *Modern Diffraction and Imaging Technique in Materials Science* p 399 Eds. S Amelinckx, R Gevers and J Van Landuyt North-Holland Amsterdam. Still the best reference because no one has really done anything of significance with Kikuchi patterns in TEM since Gareth Thomas, 40 years ago (check out the other references below).

SOME HISTORY AND APPLICATION

Christenson, KK and Eades, JA 1988 *Skew Thoughts on Parallelism* Ultramicroscopy **26** 113–132.

Dingley, DJ 1984 *On-Line Determination of Crystal Orientation and Texture Determination in an SEM*. Proc. Royal Microsc. Soc. **19** 74–75. The idea of texture mapping developed for the SEM can be applied to the TEM.

Dingley, DJ 2004 *Progressive Steps in the Development of Electron Backscatter Diffraction and Orientation Imaging Microscopy* J. Microsc. **213** 214–224.
Johari, O and Thomas, G 1969 *The Stereographic Projection and its Applications* in *Techniques of Metals Research* Ed. RF Bunshah Interscience New York.
Kikuchi, S 1928 *Diffraction of Cathode Rays by Mica* Japan J. Phys. **5** 83–96.
Levine, E, Bell, WL and Thomas, G 1966 *Further Applications of Kikuchi Diffraction Patterns; Kikuchi Maps* Appl. Phys. **37** 2141–2148.
Okamoto, PR, Levine, E and Thomas, G 1967 *Kikuchi Maps for H.C.P. and B.C.C. crystals* J. Appl. Phys. **38** 289–296.
Ryder, PL and Pitsch, W 1968 *On the Accuracy of Orientation Determination by Selected Area Electron Diffraction* Phil. Mag. **18** 807–816.
Tan, TY, Bell, WL and Thomas, G 1971 *Crystal Thickness Dependence of Kikuchi Line Spacing* Phil Mag. **24** 417–424.

URLS

1) http://cimewww.epfl.ch/EMYP/comp_sim.html

THE COMPANION TEXT

The main chapters in the companion text that relate to this topic are those on CBED and EFTEM.

SELF-ASSESSMENT QUESTIONS

Q19.1 When viewing different regions of your specimen, the intensity of the Kikuchi lines changes. Could the reason be the variation in thickness?
Q19.2 Why is the Kikuchi line nearer 000 brighter than its partner that is farther away?
Q19.3 You record a series of DPs as you tilt along a Kikuchi band. You paste the DPs together but the Kikuchi lines appear to be slightly curved Kikuchi lines, but Kikuchi lines are drawn straight. Explain.
Q19.4 When viewing another DP, a pair of parallel lines is present where one line is dark and the other is bright. Why does this happen, and how do we name each line?
Q19.5 You're writing your dissertation on the beach in Aruba so you don't have crystallography software available but the crucial DP of a certain fcc specimen stored on your laptop is only showing Kikuchi lines. Can you determine the orientation? If so, how can you do it?
Q19.6 Where is the **g** Kikuchi line relative to O and G if the excitation error, $\mathbf{s_g}$, is less than zero?
Q19.7 How does the distance between Kikuchi lines vary with specimen thickness?
Q19.8 How accurately can you determine orientations using Kikuchi lines?
Q19.9 Will a conventional TEM with a LaB_6 filament give better Kikuchi lines than a new FEGTEM at the same orientation and thickness?
Q19.10 We say that Kikuchi lines arise due to incoherently scattered electrons? This statement is a little oversimplified. Why?
Q19.11 Why are Kikuchi patterns used for setting the value of **s**?
Q19.12 What are Kossel cones?
Q19.13 What is the distance between a pair of Kikuchi lines?
Q19.14 Can you just read off **s** from where the Kikuchi line cuts the systematic row?
Q19.15 Why is there an ideal thickness for a specimen when viewing Kikuchi diffraction?
Q19.16 How can we trace the location of a plane from Kikuchi lines?
Q19.17 Briefly describe how you can find poles using Kikuchi lines.
Q19.18 Is EBSD possible in the TEM?
Q19.19 What is the distance in reciprocal space between the $-5\mathbf{g}$ and $+5\mathbf{g}$ Kikuchi lines?
Q19.20 How do HOLZ lines and Kikuchi lines differ? (Read Chapters 20 and 21 before answering this.)
Q19.21 Construct a Kikuchi map where the [001] pole is exactly on the optic axis.
Q19.22 Why do we only need the Kikuchi map for the [001], [101] and [111] triangle in fcc crystals but have to map much more of reciprocal space for hcp, and what is the largest area we would have to map for any crystal?

TEXT-SPECIFIC QUESTIONS

T19.1 Assuming that Figure 19.1 was obtained from a cubic material, determine the approximate orientation of the specimen.
T19.2 Redraw Figure 19.4A for the [011] and [111] poles but arrange for two low-index reflections to be excited in each figure.
T19.3 Consider Figure 19.6. Sketch and label the Kikuchi bands which pass through the 115 pole.
T19.4 Using Figure 19.6 draw consistent DPs for the 102, 116 and 013 poles as you would expect to see them as you tilt your fcc sample. (So you have to align them appropriately too.)

T19.5 Using Figure 19.7 draw consistent DPs for the $1\bar{2}13$, $1\bar{1}02$ and $0\bar{1}12$ poles as you would expect to see them as you tilt your hcp sample. (So you have to align them appropriately too.)

T19.6 In Figure 19.10, determine what the pole is and how far it is inclined relative to the electron beam. How would you tilt the sample to bring P onto the optic axis (assuming O is on the optic axis)?

T19.7 Consider Figure 19.10. Identify and index 10 pairs of Kikuchi lines (even if you can only see one of the lines).

T19.8 In Figure 19.11, where are the diffracting planes? Why can we see the Ewald sphere in two places? Which one is correct as the diagram is drawn?

T19.9 Sketch Figure 19.7 for Be showing the $1\bar{1}02$, $1\bar{2}13$, $0\bar{2}23$ and $\bar{1}\bar{1}23$ poles. Now superimpose on this figure the one for Ti as if the Ti had grown in perfect alignment on 0001 Be.

T19.10 Choose a 010 sample of olivine and construct the Kikuchi pattern to a radius of 45° about this pole. Label the Kikuchi bands and sketch the main DPs you will find. (You should use the Web or ICDD files to help you with this question.)

T19.11 An Al-crystal (fcc) is observed exactly along a [011] direction. Draw the corresponding DP with the associated Kikuchi lines (bands). After a small tilt of the crystal, the Kikuchi lines pass through three of the low-index reflections. How far has the crystal been tilted and what was the tilt axis? The lattice constant for aluminum is 0.405 nm. The wavelength for the electrons is 0.0025 nm. (Courtesy Anders Tholen.)

T19.12 Explain how you would deduce the accelerating voltage of the TEM using a DP from Si.